

Optimal scheduling of flexible thermal power plants with lifetime enhancement under uncertainty

Jairo Rúa^{a,*}, Adriaen Verheyleweghen^b, Johannes Jäschke^b, Lars O. Nord^a

^a Department of Energy and Process Engineering, Norwegian University of Science and Technology, Trondheim, Norway

^b Department of Chemical Engineering, Norwegian University of Science and Technology, Trondheim, Norway

ARTICLE INFO

Keywords:

Combined cycle gas turbine (CCGT)
Power system economic dispatch
Robust optimisation
Flexible operation
Dynamic modelling and simulation
Maintenance scheduling
Prognosis and reliability

ABSTRACT

Renewable energy sources have been the focal point to decarbonise the power sector. The large deployment of these intermittent power generation units requires mechanisms to balance the grid. Thermal power plants can provide this service by increasing the number of start-ups, shut-downs, and intraday ramps at the expense of higher deterioration in critical equipment, including high-pressure steam drums, turbine rotors and blades, and high-temperature heat exchangers and pipes. This work proposes a method to formulate the power generation scheduling of thermal power plants as a stochastic optimisation problem with limitations on the maximum damage in critical components. This method models the uncertainty associated with intermittent power generation from renewable sources with a scenario-tree whilst computing the deterioration of the equipment in each scenario to limit the maximum damage. Scheduling of a flexible natural gas combined cycle demonstrated how this methodology can reduce the deterioration of the superheating heat exchanger of the power plant with minimum detriment in power generation and revenue. Furthermore, the effect of the design temperature of the material on the total damage was analysed for a broad range of temperatures and operating profiles, showing how adequate selection of design temperature can reduce the deterioration of the equipment and enhance its lifetime.

1. Introduction

The decarbonisation of the power sector is a fundamental measure to reduce global anthropogenic greenhouse gas emissions and mitigate climate change [1,2]. There exists a broad portfolio of technologies that can deliver low-carbon electricity whilst meeting the increasing power demand associated with the growing population and electrification of other economic sectors. Among the different available alternatives, renewable energy sources, mainly wind and solar, have concentrated most of the efforts to reduce CO₂ emissions in this sector [2]. However, it is also recognised that the intermittent power generation nature of these renewable energy sources requires a heterogeneous and flexible power system to balance such variability and guarantee reliable, clean and efficient generation of electricity [3–5].

Thermal power plants, especially natural gas combined cycles (NGCCs), are expected to play a fundamental role in the future power sector since they can accommodate large power fluctuations in a short period of time [6,7]. These power plants are thus arguably considered as an important complement for intermittent renewable energy sources.

Furthermore, if carbon capture and storage (CCS) is integrated with thermal power plants, low carbon electricity can be provided whilst balancing the power grid [8].

In a power system dominated by rapid and large deployment of renewable energy, thermal power plants will face more frequent start-ups and shut-downs, and faster ramping rates in order to balance the grid [6,9,10]. This aggressive operation will originate larger and more periodic thermal and mechanical stresses in the equipment of thermal power plants, which may lead to irreversible damages if the maximum stress limits of the material are exceeded. High-pressure steam drums, boiler tubes with superheated and reheated steam, headers, and first-stage rotor disks, blades and casings of high-pressure steam turbines are some of the equipment that endures the highest stress levels during start-ups, shut-downs and ramping operation [11–19].

There are several procedures and control methodologies to avoid exceeding the maximum allowable stresses in these critical components. Bypassing a fraction of the flue gas is a common and effective start-up procedure to limit the maximum stress in the steam drums and boiler tubes during the start-up of a power plant, as it reduces the temperature gradient in the walls and hence the effective stress peaks [13,15]. This

* Corresponding author.

E-mail addresses: jairo.r.pazos@ntnu.no (J. Rúa), lars.nord@ntnu.no (L.O. Nord).

Nomenclature			
<i>Latin symbols</i>		σ	Stress [MPa]
a	Coefficients of polynomials [-]	σ'_f	Tensile strength coefficient [MPa]
b	Coefficients of polynomials [-]	ν	Poisson's ratio [-]
C	Specific heat capacity [J/kg K]	ε	Strain [-]
D	Damage [-]	ε'_f	Ductility coefficient [-]
d	Uncertainty realisation [-]	<i>Subscripts</i>	
E	Young's Modulus [MPa]	θ	Tangential direction
E^*	Non-anticipativity matrix [-]	creep	Creep damage
h	Convection coefficient [W/m ² K]	design	Design
k	Heat conduction coefficient [W/m K]	e	Elastic
M	Number of uncertainty realisations [-]	eff	Effective stress
N_r	Robust time horizon [-]	exp	Experimental
N	Time horizon [-]	f	Failure
n	Number of cycles [-]	fatigue	Fatigue damage
P	Price [-]	i	Inner radius
p	Pressure [MPa]	ineq	Inequality
r	Radius m	init	Initial conditions
S	Number of scenarios [-]	m	Metal
T^*	Temperature deviation from design [°C]	max	Maximum
T	Temperature [°C]	o	Outer radius
t	Time [s]	oper	Operation
u	Manipulated variable [-]	p	Plastic
x	Estimated thermodynamic variables [-]	r	Radial direction
<i>Greek symbols</i>		wall	Wall of the tubes
α	Thermal diffusivity [m ² /s]	z	Longitudinal direction
α^*	Thermal expansion coefficient [1/K]	<i>Superscripts</i>	
$\Delta\varepsilon$	Strain amplitude [m]	b	Elastic fitting parameter
ω	Scenario weights [-]	c	Plastic fitting parameter
ρ	Density [kg/m ³]	low	Lower bound
		up	Upper bound

enables the control of the heating rate within the boiler, which can be progressively modified to achieve faster warm-ups with limited maximum stresses [16,17]. A similar procedure is followed in the steam turbine, where the steam is initially bypassed to accommodate the warm up of the steam turbine and avoid excessively high thermal stresses [14,15,19]. The maximum allowable stress in this critical equipment can also be embedded in optimisation-based control strategies so the constraints imposed by the material can be considered when computing the control actions [20,21]. Therefore, this type of methodologies allow the computation of optimal control sequences that never exceed the maximum stress levels the equipment can tolerate and enhance the flexible operation of thermal power plants.

Nevertheless, regular operation induces damage in the equipment of thermal power plants that reduces its lifetime even if these procedures and control strategies keep the stress levels within safe limits. Creep and fatigue are arguably the main damage mechanisms that initiate and grow cracks in highly loaded components, ultimately leading to lack of reliability and failures due to fractures or large deformations [11,12]. Creep refers to the damage originated by the continuous operation at specific temperature and stress levels, which can result in deformations in the short term, and crack growth and cavitation in the long term [12,22,23]. Fatigue is the progressive and persistent structural damage originating from cyclic loading in the material [11,12,24]. Low-cycle fatigue occurs in the components of thermal power plants that operate at high temperature and pressure (e.g. headers, superheater and reheater tubes, steam turbine rotors), whereas high-cycle fatigue affects the equipment that experiences vibration (e.g. turbomachinery components) [11,12,25]. Additional damage phenomena that can affect the residual lifetime operation of thermal power plants are corrosion, embrittlement, oxidation, pitting and erosion [11].

Damage and degradation of thermal power plant components are normally generated by a combination of mechanisms. Barella et al. [26] studied the failure of a steam turbine rotor with finite element methods (FEMs), concluding that high thermal stress concentration initiated the cracks that were propagated by mechanical fatigue. Similar crack developments can be observed in the failure of steam turbine blades [27]. Mechanical fatigue is also the propagation mechanism of the crack, whereas crack initiation can occur by corrosion. Creep is another damage phenomena that can initiate cracks in the rotors of steam turbines because of the high temperatures and stresses this type of components must withstand. Thus, the combination of creep and fatigue is a common failure mechanism in steam turbines [12,28,29]. Creep and creep-fatigue damage is also typical in the tubes of superheaters and reheaters because of their operating conditions, with high inner and outer temperatures and high pressure steam flowing inside the tubes. Furthermore, these components experience large and frequent temperature gradients owing to the ramping operation of thermal power plants, which generates larger stresses and more cyclic loading that enhance the damage through creep and thermo-mechanical fatigue [30]. The operation profile hence influences the damage in the equipment and its lifetime reduction. Benato et al. [31,32] compared different flexible operation profiles for a three pressure level heat recovery steam generator (HRSG) and a combined cycle, and observed that the faster ramp rates substantially increased the degradation of the superheater tubes. These components are also sensitive to the composition of the exhaust gas as it may contain chemical components that generate hot corrosion in the presence of certain elements, which results in wall thinning and premature failure without the adequate maintenance [33].

Whilst the limitation of maximum stress levels occurs in the short timescales (i.e. orders of seconds and minutes) and depends on the

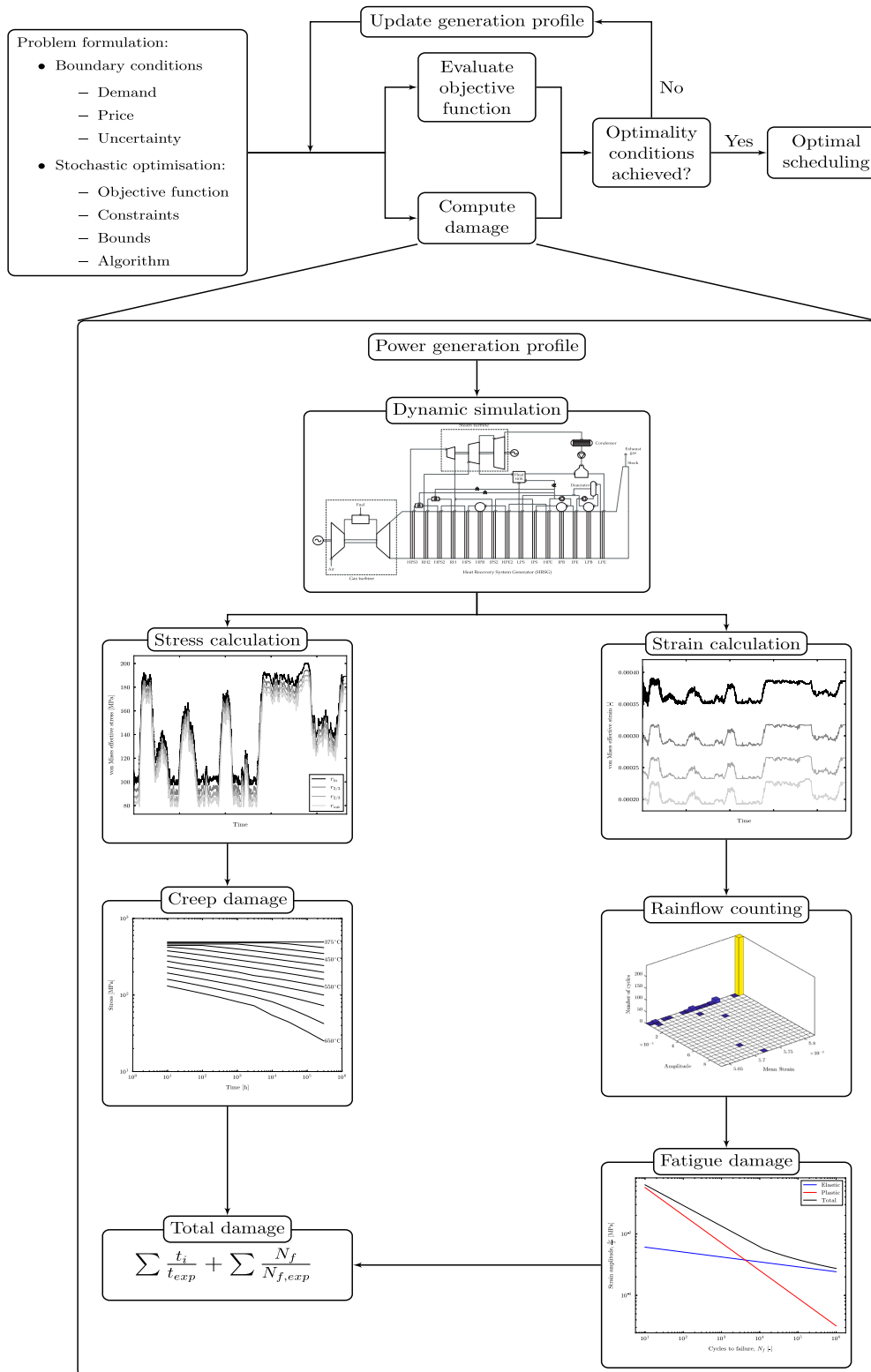


Fig. 1. Method to optimally schedule the power generation profile of thermal power plants with lifetime enhancement under uncertainty.

regulatory and supervisory control layers [20,21], the evaluation of creep and fatigue damage and the associated reduction of operational lifetime in critical equipment owing to the operation of thermal power plants befall in longer time scales (i.e. days, weeks and months), or once the failure has already occurred. Damage in critical equipment may also be monitored online to quantify its deterioration and allow more

accurate assessments of possible repairs and maintenance [28,34]. Nevertheless, online monitoring of the damage is only valid for failure prevention since the power generation profile, which determines the operation and hence the damage in the equipment of thermal power plants, is normally defined one day ahead in deregulated power markets.

Therefore, scheduling of daily and weekly operation of thermal

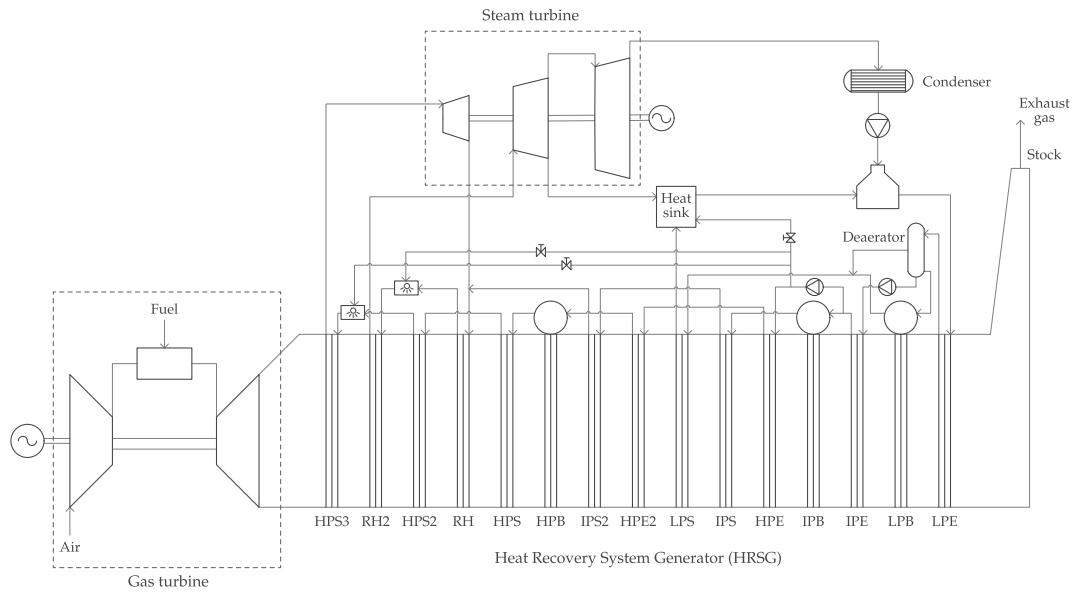


Fig. 2. Process model of the natural gas combined cycle. The nomenclature in the HRSG is as follows: E: Economiser, B: Boiler, S: Superheater, R: Reheater P: Pressure, L: Low, I: Intermediate, H: High.

power plants in power markets with large shares of renewable energy confronts three main challenges: (1) adapt the operation profile to intermittent power generation from renewable energy sources and demand variations, (2) consider the uncertainty associated with this type of technology, and (3) limit the deterioration of critical equipment because of the flexible operation required to balance power generation and demand. Traditional scheduling methods focus on point (1), with modern approaches progressively including the uncertainty from renewable power generation and demand fluctuation [35–37], whereas damage analysis is decoupled from the scheduling stage and carried out once the fault has already occurred.

This study presents a methodology that addresses these three requirements. In this scheduling strategy, power generation profiles of thermal power plants are the result of an optimisation problem where the maximum deterioration of the equipment by different damage phenomena is limited. Furthermore, this optimisation is formulated as a scenario-tree stochastic optimisation problem to consider the uncertainty associated with the intermittent renewable energy sources. Thus, the main contribution of this work is the combination of the scheduling process with the uncertainty associated with renewable energy sources and the deterioration of the equipment in a stochastic optimisation framework. This approach enables thermal power plants to balance the grid under different scenarios whilst enhancing the lifetime of sensitive equipment and maximising their economical performance.

This methodology involves several models that are merged in an optimisation framework, whereas its formulation allows including different types of uncertainty and deterioration mechanisms. The structure of this work follows a modular approach to show how this methodology can be easily adapted to different applications and scenarios. Section 2 describes the overall method and presents the different models required during the optimisation to estimate the dynamic power plant behaviour, the stress and strain arising in different equipment, and the damage caused by different phenomena. Section 3 presents the mathematical formulation of the proposed scheduling method, and details how these models are combined in a scenario-tree stochastic optimisation problem that limits the damage in the equipment. A case study analysed in Section 4 illustrates the application of the proposed methodology to the scheduling of a day-ahead power generation profile for a natural gas combined cycle and discusses the importance of adequate selection of design temperatures in the equipment. Conclusions and final remarks are included in Section 5.

2. Method for stochastic scheduling with lifetime enhancement

Flexible operation of thermal power plants may result in a substantial reduction of their operational lifetime. It is thus fundamental to consider the deterioration generated by this type of operation to assess the economic viability of these power generation systems. The methodology presented in this paper aims at limiting the damage in the components of a power plant whilst optimally scheduling the power generation profile. Moreover, the uncertainty in the power demand and the power generation from intermittent renewable energy sources is considered by formulating the scheduling of power generation as a stochastic optimisation problem. Fig. 1 summarises the methodology proposed in this study.

In deregulated power markets, one-day ahead predictions of the demand are available so the power producers can schedule their operation and offer a selling price for the produced electricity. The proposed methodology considers hence that an estimation of the demand and the uncertainty attached to this prediction are known. In addition, a price profile for the given demand is also assumed, albeit several prices with different uncertainties may be considered to cover a broad range of scenarios where the plant operator can adjust the electricity price to obtain more revenue or be more competitive. These demand and price profiles and their associated uncertainties are used to define a stochastic optimisation problem to schedule a power generation profile that maximises revenue and does not exceed the maximum allowable damage in the components of the thermal power plant.

In this optimisation process, the deterioration of the different components of the power plant is a constraint. Therefore, the different power generation profiles computed by the optimisation algorithm are used to calculate the damage in specific equipment and check if the constraints are satisfied (see Fig. 1). The damage calculation is a sequential procedure where the possible optimal power generation profile is utilised to carry out a dynamic simulation that attempts to recreate the behaviour of an actual thermal power plant. Stresses and strains throughout the operation period can thus be obtained for the equipment of interest. Damage is subsequently computed by considering these stresses and strains and the adequate experimental data for the material of the considered equipment. The total deterioration owing to the different damage mechanisms is the result of a linear summation rule. This procedure to compute the damage generated by different phenomena from the operation profile of a thermal power plant is illustrated in Fig. 1.

Damage estimation is a procedure that requires several types of models. The remainder of this section includes the description of the dynamic models that replicate the operation of an actual thermal power plant in Section 2.1, the modelling approach to compute the stresses and strains in the equipment in Section 2.2, and the methods to estimate the damage depending on different mechanisms in Section 2.3.

2.1. Dynamic modelling of a natural gas combined cycle

This study considers a natural gas combined cycle with three-pressure levels and reheating. This type of thermal power plant is the most efficient, flexible and less polluting fossil-fueled plant available [18,38]. Thus, they are expected to ramp more frequently to balance the intermittent power generation from renewable energy sources [6,7]. Deterioration of these thermal power plants may become an issue without the adequate scheduling, and hence a modern NGCC is used to demonstrate the application of the proposed methodology.

The design of the NGCC was performed with GT PRO [39] because it provides details about the material of the equipment, the geometry and dimensions of individual components, maps of performance for the pumps, and experimental data for the exhaust conditions and power generation of the gas turbine. Fig. 2 represents the process layout of the NGCC considered in this work. The dynamic model of the NGCC was developed with the specialised thermal power library [40] in the software Dymola [41], which is based on the Modelica language [42]. This model relies on conservation laws, detailed heat transfer and pressure drop correlations, maps of performance and experimental data to adequately simulate the dynamic operation of the NGCC. A thorough description of the modelling principles and validation results of this dynamic model can be found in the work by Montañés et al. [43].

High-fidelity dynamic models representing large energy systems are not suitable for optimisation because of their high computational cost. Simplified models that capture the dynamic behaviour of thermodynamic variables of interest must thus be used instead. System identification can be implemented to obtain dynamic data-based models that predict the overall transient performance of specific variables [44]. However, since scheduling captures the long-term dynamic behaviour of thermal power plants, quasi-steady state models may be used without excessive loss of accuracy and standard regression approaches can be applied.

Temperatures and pressures in the equipment of interest are normally the thermodynamic variables estimated by simplified models, as they are the boundary conditions of the stress models that allow computation of creep and fatigue damage. If other deterioration mechanisms such as hot corrosion are considered, simplified models to estimate the composition of specific chemical components in the flue gas could also be developed and implemented in the proposed methodology. In addition, a simplified model for predicting the power generation of the thermal power plant is also needed.

The tubes in the superheating section of the heat-recovery steam generator (HRSG) of the NGCC are considered. Creep is a major issue for this type of components because they experience many drastic operation changes during regular operation of NGCCs as a result of the frequent ramping, start-ups and shut-downs [11,12]. Therefore, the tubes in the superheaters are a suitable and illustrative example to demonstrate the lifetime enhancement capability of the methodology proposed in this work.

Table 1
Fitting parameters of the simplified models and coefficient of determination R^2 .

x	a	b	$R^2[\%]$
Power	90	5.25	99.95
Inner pressure	6.48	0.08	99.88
Inner temperature	377.17	1.83	95.58
Outer temperature	768.57	-1.45	93.43

This component only requires simplified models to predict the inner temperature and pressure, and outer temperature since creep is the unique failure phenomenon. The outlet pressure in the HRSG is almost constant because of the minimal changes in the pressure drop of the exhaust gas. A direct relation may be established between the gas turbine load and the quasi-steady state value of these variables. Therefore, linear polynomials with the structure presented in Eq. (1) lead to adequate estimations, where x represents the different predicted variables (i.e. mechanical power generation, and inner and outer pressure and temperature in the superheated tubes), u is the manipulated variable, which is the gas turbine load as it dictates the operation profile of the NGCC, and parameters a and b are fitted to the high-fidelity model for each variable. Table 1 summarises the fitting parameters of each variable and presents the coefficient of determination R^2 that measures the agreement between the high-fidelity and simplified models. Fig. A.11 presents a comparison between the high-fidelity and simplified models for the considered temperatures and pressure.

$$x = a + bu \tag{1}$$

2.2. Stress and strain modelling

In thermal power plants, there are several components that must withstand high temperatures and pressures. These operating conditions originate both thermal and mechanical stresses, which lead to the progressive deterioration of the equipment. Thermal stresses depend on the temperature gradient along the wall of the component and the design temperature of the material, whereas the mechanical contribution is proportional to the applied mechanical forces (e.g. pressure or centrifugal force). The temperature distribution along the wall of any circular equipment (e.g. pipes, tubes or rotors) is obtained with the heat equation assuming that heat transfer occurs exclusively in the radial direction:

$$\frac{1}{r} \frac{\partial}{\partial r} \left(r \frac{\partial T^*}{\partial r} \right) = \frac{1}{\alpha} \frac{\partial T^*}{\partial t} \tag{2}$$

where r is a generic radius, α is the thermal diffusivity of the material, and T^* refers to the temperature difference respect to the design temperature of the equipment.

The temperatures in the inner and outer surfaces are the boundary conditions that define the temperature distribution in the wall. Thermal stresses can hence be computed considering this temperature profile. The method to calculate these stresses depends on the geometry of the component. Plane strain is a suitable modelling approach for equipment where the longitudinal dimension is notably larger than in the radial or tangential directions [45]. Pipes, drums, headers, downcomers and any component with a cylindrical shape can be modelled under the plain strain assumption. In contrast, if the longitudinal dimension is almost negligible compared to the other two dimensions, plane stress can be assumed to model the stress [45]. This modelling approach describes the stresses that arise in the rotor disks of the steam turbines (see, e.g., the work by Rúa et al. [20,21]). More detailed and intricate stress modelling approaches, or even finite element methods (FEMs), may be necessary to determine the stress generated in complex geometries such as turbine blades.

$$\begin{aligned} \sigma_r = & \left(1 - \frac{r_i^2}{r^2} \right) \frac{E \alpha^*}{(1+\nu)(1-2\nu)} \int_{r_i}^{r_o} r T^* dr - \frac{E \alpha^*}{(1-\nu)} \int_{r_i}^r r T^* dr \\ & + \left[\frac{r_o^2 r_i^2}{(r_o^2 - r_i^2) r^2} - \frac{r_o^2}{(r_o^2 - r_i^2)} \right] (p_o - p_i) - p_i \end{aligned} \tag{3a}$$

$$\begin{aligned} \sigma_\theta = & \left(1 + \frac{r_i^2}{r^2} \right) \frac{E \alpha^*}{(1-\nu)(r_o^2 - r_i^2)} \int_{r_i}^{r_o} r T^* dr + \frac{E \alpha^*}{1-\nu} \left(\frac{1}{r^2} \int_{r_i}^r r T^* dr - T^* \right) \\ & + \left[\frac{r_o^2 r_i^2}{(r_o^2 - r_i^2) r^2} + \frac{r_o^2}{(r_o^2 - r_i^2)} \right] (p_i - p_o) - p_i \end{aligned} \tag{3b}$$

$$\sigma_z = \frac{2\nu E \alpha^*}{(r_o^2 - r_i^2)(1 - \nu)} \int_{r_i}^{r_o} r T^* dr - \frac{E \alpha^*}{1 - \nu} T^* + p_i \left(\frac{2\nu r_o^2}{r_o^2 - r_i^2} - 2\nu \right) - p_o \frac{2\nu r_o^2}{r_o^2 - r_i^2} \quad (3c)$$

Both modelling approaches are based on the stress–strain constitutive equations, the strain–displacement relations and the radial equilibrium equation. Expressions for the principal stress components are obtained if these relations are combined and the ordinary differential equation that determines the displacement is solved analytically. The mechanical stresses enter these expressions by including the inner and outer pressure as boundary conditions and the centrifugal force as an additional term in the radial equilibrium equation. A detailed development of the equations describing the principal stresses under the assumptions of plane strain and strain can be found in the work by Rúa et al. [20,21]. Eq. (3) defines the principal stress components under the plane strain assumption, which is the modelling approach that describes the stresses arising in the tubes of the superheater. Thermal stresses arise when the temperature distribution in the wall is different from the design temperature at which the component was produced. Therefore, the temperature T^* in any stress or strain expression refers to the deviation with respect to that initial temperature.

The von Mises equivalent, or effective, stress is a scalar measure that represents the overall effect of the principal stress components. This variable, defined in Eq. (4), is therefore suitable to estimate the overall damage induced by a power generation profile.

$$\sigma_{\text{eff}}^2 = \sigma_r^2 + \sigma_\theta^2 + \sigma_z^2 - (\sigma_r \sigma_\theta + \sigma_\theta \sigma_z + \sigma_z \sigma_r) \quad (4)$$

Strains are computed from the temperature profile along the wall, the principal stress components and the stress–strain constitutive relations [45]. If plane strain is assumed to model the stresses and strains in a component, the strain in the longitudinal direction is zero. Thus, the strains for the tubes in the superheater are:

$$\epsilon_r = \frac{1}{E} (\sigma_r - \nu(\sigma_\theta + \sigma_z)) - \alpha^* T^* \quad (5a)$$

$$\epsilon_\theta = \frac{1}{E} (\sigma_\theta - \nu(\sigma_r + \sigma_z)) - \alpha^* T^* \quad (5b)$$

Similar to the stress models, an overall effective strain can be defined following the von Mises criteria [24]:

$$\epsilon_{\text{eff}}^2 = \epsilon_r^2 + \epsilon_\theta^2 + \epsilon_z^2 - (\epsilon_r \epsilon_\theta + \epsilon_\theta \epsilon_z + \epsilon_z \epsilon_r) \quad (6)$$

These temperature, stress and strain models were validated using high-fidelity finite element methods for the same operating conditions. Fig. A.12 illustrates the agreement between the stresses and strains of the proposed models and the FEM analysis.

2.3. Damage estimation methods

Deterioration of the equipment in thermal power plants occurs as a result of a combination of different damage phenomena [11,12]. Creep and low cycle fatigue are arguably the most common and relevant failure mechanisms caused by the cyclic operation of flexible power plants [12,31,32]. Therefore, this work describes the main methods to estimate the deterioration caused by both phenomena.

The calculation of damage relies on experimental data obtained by the repetition of different tests in samples of specific materials [11,24]. Different procedures are hence applied to obtain this data depending on the damage mechanisms. Creep is normally computed with charts as in Fig. 3 that relate the operating stress level and temperature with the maximum operating time at these conditions before failure [11]. Thus, the total creep damage generated during the operation of a thermal power plant is:

$$D_{\text{creep}} = \sum_{i=1}^m \frac{t_{\text{oper}}}{t_{\text{exp}}} \quad (7)$$

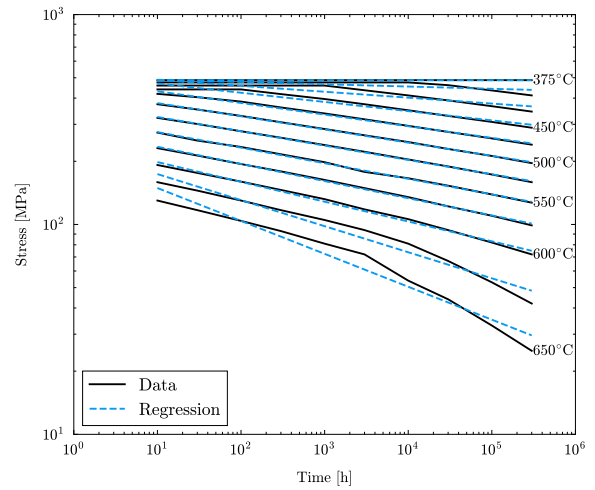


Fig. 3. Diagram with experimental data to estimate the creep damage. The black lines represent the data obtained experimentally whereas the blue lines are linear regression models used during the optimisation.

where t_{oper} is the time that a component of the power plant operates at a specific temperature and stress level, t_{exp} is the maximum operational time obtained experimentally at those levels, and m is the number of considered operation points.

Experimental data are discrete. Therefore, the computation of creep damage given the operating temperature and stress profiles from the models described in Section 2.1 and Section 2.2, respectively, requires a two-dimensional interpolation to obtain the experimental time that the equipment can operate at such conditions. Interpolation is not suitable for optimisation since different iterations may lead to points that lay outside the experimental data set and hence to convergence issues. Linear models of the experimental data were thus developed by standard least-squares to have continuous models that ease the convergence of the optimisation. The creep data estimated by the regression models is compared to the experimental data in Fig. 3.

Fatigue depends on the cyclic loading that the equipment undergoes during regular operation. Rotating machinery can experience vibrations and hence high cycle fatigue. In contrast, high-temperature components in thermal power plants suffer low cycle fatigue because of the low frequency of the operation changes [11,12,24,31,32]. Damage originated by both fatigue mechanisms is also calculated with procedures based on experimental data, although stress profiles are normally used to correlate the operating conditions with the high cycle fatigue deterioration and strain profiles to compute the low cycle fatigue damage [24,46].

The stress and strain profiles are not uniform since they depend on the operation of the thermal power plants. However, the experimental data utilised to compute the fatigue damage is obtained by applying uniform cyclic loading to the samples of material. Standardisation techniques that transform the variable spectrum of stresses and strains into uniform loading profiles are therefore required to calculate the fatigue damage. Rainflow counting is a procedure that extracts the hysteresis cycles from the loading spectrum and generates uniform loading cycles from non-uniform stress and strain profiles [24,47–50]. This results in a set of amplitudes and mean stress or strain ranges with an associated number of cycles (see Fig. 1). The fatigue damage is calculated by comparing the number of cycles obtained from the rainflow counting procedure and the experimental maximum number of cycles for a specific amplitude and mean stress/strain [24,46]. Eq. (8) represents the computation of the fatigue damage following the linear cumulative damage hypothesis formulated by Miner–Palmgren [46,51,52]:

$$D_{\text{fatigue}} = \sum_{i=1}^{n_r} \frac{n_{\text{oper}}}{n_f} \quad (8)$$

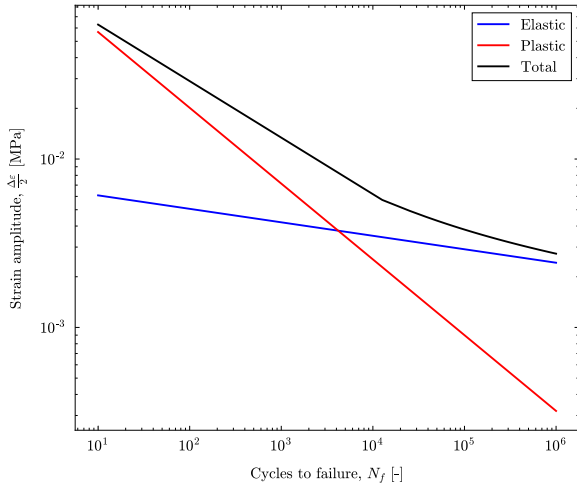


Fig. 4. Diagram with experimental data to estimate the fatigue damage. The black line represents the maximum experimental number of cycles to failure given that a strain amplitude is a combination of elastic and plastic effects.

where n_{oper} is the number of operation cycles for a given strain amplitude and mean strain, n_r is the number of the different considered ranges, and n_f is the experimental data for the maximum number of cycles before failure. This experimental data is normally represented by the Coffin-Manson equation [24,46]:

$$\frac{\Delta \varepsilon}{2} = \frac{\Delta \varepsilon_e}{2} + \frac{\Delta \varepsilon_p}{2} = \frac{\sigma'_f}{E} (2n_f)^b + \varepsilon'_f (2n_f)^c \quad (9)$$

with σ'_f and ε'_f being, respectively, the tensile strength and ductility coefficient scaled to fit the experimental data, and b and c are fitting parameters. The elastic contribution to the overall strain amplitude is $\Delta \varepsilon_e/2$, whereas $\Delta \varepsilon_p/2$ is the plastic component. Fig. 4 illustrates the experimental fatigue data fitted to the Coffin-Manson equation.

Experimental fatigue data represents the effect of uniaxial loading in

the deterioration of samples of a specific material. The equipment of thermal power plants is however exposed to multiaxial loading. Therefore, to estimate the fatigue damage with uniaxial experimental data, the effective values of the stress and strain defined in Eqs. (4) and (6) are used [24,53,54]. This allows the utilisation of available experimental uniaxial data to compute the fatigue damage from complex multiaxial loading.

The total damage of a component results from the summation of the individual contributions of the different damage phenomena:

$$D = D_{creep} + D_{fatigue} \quad (10)$$

This method to compute the deterioration of the equipment in thermal power plants eases the inclusion of different damage mechanisms. For instance, hot corrosion could be added by developing a model that predicted the deposition of eroding elements in the equipment and an expression that correlated this deposition with the operating conditions and the generated damage.

3. Scheduling as a stochastic optimisation problem

Scheduling of thermal power plants in deregulated markets is a challenging procedure because of the large deployment of intermittent renewable energy sources. The intrinsic uncertainty associated with the power generation from solar and wind power sources imposes drastic operation profiles on traditional thermal power plants to balance the grid. This work proposes the utilisation of scenario-based multistage optimisation to consider the uncertainty associated with renewable power generation and schedule the operation of flexible thermal power plants whilst limiting the maximum damage in their critical components. The scheduling problem becomes hence a stochastic optimisation problem where the different scenarios represent the uncertainty in the power demand and the deterioration of the equipment is a constraint. This section describes the mathematical formulation of the method illustrated in Fig. 1.

Scenario-based multistage optimisation models the uncertainty of a process as discrete realisations of a probability density function representing such uncertainty, considers the different possible combinations of these realisations, and integrates them in an optimisation framework that

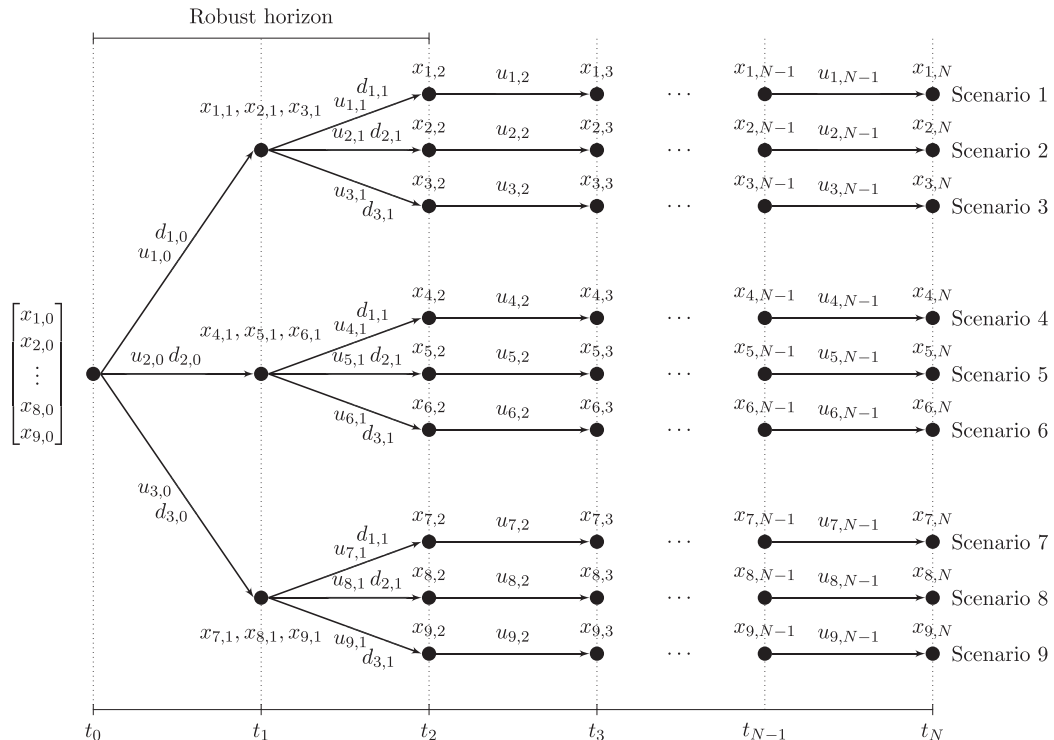


Fig. 5. Schematic representation of a scenario-tree with $M = 3$ uncertainty realisations and a robust time horizon $N_r = 2$.

aims at finding the optimal solution of all possible uncertain scenarios [55]. Therefore, its application to the one-day ahead scheduling of power generation from thermal power plants in flexible power markets may enhance the optimal utilisation of this type of power plants. Furthermore, since the scheduling problem is expressed as a stochastic optimisation problem, the maximum damage induced by the regular operation of the power plant can be included as a constraint, which may expand the lifetime of traditional thermal power plants. Fig. 5 represents the scenario-tree evolution embedded in the optimisation problem. Given a known initial operation point, M different uncertainty realisations, d , consider the power generation uncertainty of the intermittent renewable energy sources. These realisations represent possible power demands that the thermal power plant must balance by modifying its manipulated variable, u , which is the gas turbine load in NGCCs and the fuel input in coal and biomass power plants, to produce the adequate amount of power.

The robust time horizon, N_r , limits the extension to which the uncertainty is considered, as the size of the optimisation problem, i.e. the number of scenarios, increases exponentially, $S = M^{N_r}$, with this horizon. In contrast to design problems, where the stochastic optimisation problem is solved only once, this scheduling method may re-solve the optimisation problem continuously with updated information (e.g. every two hours). This means that it is not necessary to branch the scenario tree until the end of the prediction horizon. Instead, the expansion of the scenario tree might be stopped after a robust horizon, and from this point on consider the uncertainty unchanging. The main reasoning is that information about the far future need not be accurately represented at the time when the decision is made, because the decisions will be refined in the next optimisation, when the scheduling problem is solved again with new information.

The mathematical formulation of the scheduling problem as a scenario-tree optimisation problem is:

$$\min_{x_{i,j}, u_{i,j}} \sum_{i=1}^S \omega_i \sum_{j=0}^{N-1} \ell(x_{i,j}, u_{i,j}, P_j) \quad (11a)$$

$$\begin{aligned} &\text{subject to} \\ x_{i,0} &= x_{\text{init}} \quad \forall i \in \mathcal{S} \end{aligned} \quad (11b)$$

$$x_{i,j} = f(x_{i,j}, u_{i,j}, d_{i,j}) \quad \forall i \in \mathcal{S}, \forall j \in \mathcal{N} \quad (11c)$$

$$c_{\text{ineq}}(x_{i,j}, u_{i,j}) \leq D_{\text{max}} \quad \forall i \in \mathcal{S}, \forall j \in \mathcal{N} \quad (11d)$$

$$(x_{i,j}, u_{i,j})^{\text{low}} \leq (x_{i,j}, u_{i,j}) \leq (x_{i,j}, u_{i,j})^{\text{up}} \quad \forall i \in \mathcal{S}, \forall j \in \mathcal{N} \quad (11e)$$

$$\sum_{i=1}^S E_i^* u_i = 0 \quad \forall i \in \mathcal{S} \quad (11f)$$

where the subscripts $(\cdot)_{i,j}$ refer to the i^{th} scenario at the j^{th} sample time, \mathcal{S} is the set of scenarios $\mathcal{S} := \{1, \dots, S\}$, and \mathcal{N} denotes the set of indices j defining the sampling time such $\mathcal{N} := \{1, \dots, N\}$. The cost function in Eq. (11a) is a weighted average of the individual cost functions of each scenario, where ω_i is the coefficient that determines the weight of each scenario. Since scheduling problems aim at maximising the operating profit, the cost function is defined as:

$$\ell(x_{i,j}, u_{i,j}, P_j) = -x_{i,j}^T P_j \quad (12)$$

with P_j representing the price of the generated power and $x_{i,j}$ the scheduled power generation, which is a vector including the discrete sequence of operation points that define the quasi-steady state net power production of the NGCC throughout each scenario.

The equality constraints in Eq. (11c) ensure that the models describing the behaviour of the thermal power plant (i.e. the simplified models for power generation, inner pressure and temperature, and outer temperature in Eq. (1) and Table 1 are satisfied for all uncertainty

realisations $d_{i,j}$. In contrast to the original model predictive control application where the equality constraints predict future dynamic behaviour of the system [55], Eq. (11c) only guarantees that the solution satisfies the quasi-steady state performance of the power plant but does not include any prediction, as each point of the sequence defining the power generation profile is independent. The inequality constraints represented by Eq. (11d) include the computation of the damage in the equipment over the time horizon N and limit its value to a maximum allowable level specified by D_{max} , whereas Eq. (11e) defines the lower and upper bounds of the computed thermodynamic variables in the equipment x (i.e. temperatures, pressure and power) and the manipulated variable u . Eq. (11b) sets the initial conditions of the power plant, which are common for all scenarios.

Scenario-tree optimisations include the uncertainty in the process by the continuous branching of different scenarios. This approach hence considers a broader range of operating conditions, but it also imposes extra restrictions during the optimisation. As the disturbances associated with the uncertainty cannot be predicted, the control inputs must not anticipate them and the power plant states x in every node must be equal. This implies that the control inputs leading to a node within the robust horizon are equal for the different scenarios branching from that node [55–58]. These restrictions are the non-anticipativity constraints, and are enforced in the optimisation problem by Eq. (11f), where $u_i = [u_{i,0}, u_{i,1}, u_{i,2}, \dots, u_{i,N-1}] \in \mathbb{R}^N$.

4. Optimal scheduling of flexible natural gas combined cycles: a case study

The scheduling of a flexible NGCC was considered to illustrate the application of the methodology proposed in this work. Section 4.1 presents a case study where the maximum creep damage in the tubes of the superheater is limited whilst maximising the power generation of the NGCC. Moreover, since stress, and consequently creep damage, are profoundly affected by the design temperature of the equipment, the effect of this parameter on both effective stress and deterioration is studied for a broad range of temperatures in Section 4.2.

4.1. Optimal scheduling with lifetime enhancement

The power demand profile estimated by the grid operator and scaled to the power generation range of the actual power plant is represented in Fig. 6. This demand was simplified to a coarser profile since scheduling aims at defining overall power generation profiles and NGCCs can respond within seconds to small, unscheduled variations in power

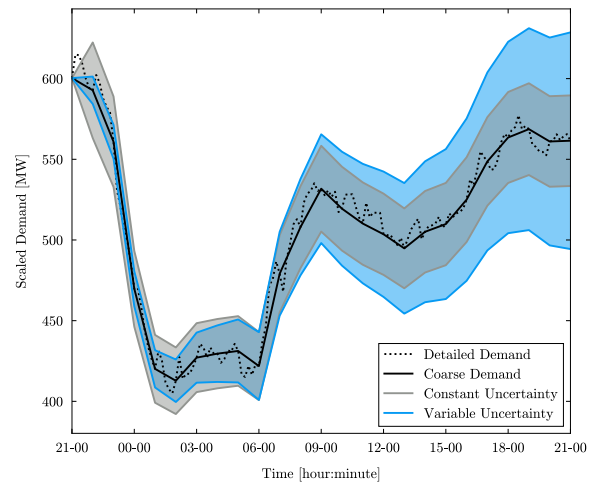


Fig. 6. Demand profile estimated in day-ahead markets with a coarse simplification and intervals for constant and increasing uncertainty.

Table 2
Physical and mechanical properties of T91 martensitic steel.

ρ [kg/m ³]	C_m [J/kgK]	k_m [W/mK]	α^* [m ² /s]	α [1/K]	E [MPa]	ν [-]	h_o [W/m ² K]	h_i [W/m ² K]
7750	770	33	5.53e-05	1.3e-5	180000	0.3	2000	400

demand [20,21]. Furthermore, Fig. 6 illustrates two different types of uncertainty that can be included in the stochastic optimisation. This work assumed a $\pm 5\%$ constant uncertainty in the estimated power demand (grey area in Fig. 6). The time and robust horizons were, respectively, 24 and 2 h, with a sampling time of 1 h, whereas 3 uncertainty realisations were considered, leading to a total of 9 scenarios that were equally weighted. Fig. 5 represents this stochastic problem for the considered realisations and robust time horizon. This number of uncertainty realisations and robust time horizon was considered a reasonable trade-off between adequate consideration of uncertainty and computational cost. The price of electricity is shown in Fig. B.13.

Scheduling of the power generation from the NGCC was first carried out *without* damage constraints to obtain an operation profile benchmark that maximised the revenue. The sequential least-squares quadratic programming (SLSQP) algorithm [59,60] included in the nonlinear optimisation package NLOPT [61] was used in the optimisation. A maximum total damage $D_{\max} = 0.00017$ was then included in the stochastic optimisation problem. This allows identifying the main restrictions imposed by the constraint in the maximum damage and points out its effect on the shape of the power generation profiles in different scenarios. This study only considers creep damage in the tubes of the superheater as this is the main deterioration mechanism in this type of components [11,12]. The material of the tubes was T91, a martensitic steel for high temperature applications with its physical and mechanical properties summarised in Table 2 [62]. The design temperature of the tubes considered in this case study was 510 °C.

The nomenclature referring to the different scenarios in the stochastic optimisation problem is based on the sequence of uncertainty realisations, where H, M and L indicate the high (105%), medium (100%) and low (95%) values of the power demand estimated by the grid operator. Since the robust time horizon considered in this work is 2, a pair of letters defines each scenario. The first letter refers to the uncertainty realisation in the first sampling time and the second letter indicates the next one. For instance, the pair HL refers to the scenario where the scheduled power considers the highest demand in the first sampling time, and the lowest in the second. Moreover, the letter X is used to indicate all uncertainty realisations (e.g. XH refers to all scenarios where the second uncertainty realisation represents the higher demand profile, independently of the first realisation).

Fig. 7 shows the scheduled power for each scenario and the time distribution of the associated wall temperature, von Mises stress and the creep damage in the tubes of the superheater. Fig. 8 represents the accumulated deterioration for the scheduled power generation profiles. The maximum damage limitation, $D_{\max} = 0.00017$, only affected the HX scenarios since they produced a higher deterioration in the unconstrained¹ case. Despite the reduction in the deterioration of the equipment to meet the maximum damage constraint could be also achieved in the final hours of operation (Fig. 7g and h), the scheduling methodology performed the entire damage reduction in the first operating period since the electricity price was lower. A change in the operation profile of the NGCC (Fig. 7a and b) lead to different operating conditions that resulted in lower temperature (Fig. 7c and d) and effective stress (Fig. 7e and f) in the wall of the superheater tubes, and hence in smaller creep damage because of the combined effect of a reduction in both variables (see Fig. 3).

Modifying the power generation profile in the HH scenario to meet

the damage constraint also affected the HM and HL scenarios. This coupling occurs because of the non-anticipativity constraints in Eq. (11f), which enforces the set of scenarios HX to coincide in the first uncertainty realisation. Therefore, all HX scenarios consider the same uncertainty level in the first sampling time of the robust horizon. The HL scenario hence changes when the constraint in the damage is imposed, albeit it had not reached this limit in the unconstrained case. This illustrates the effects of combining in a stochastic optimisation problem the damage limitation of the equipment with the uncertainty in the estimated power demand.

A comparison between the accumulated revenue for all scenarios and the unconstrained and constrained problems is presented in Fig. 9. Revenue did not change in the MX and LX scenarios since the damage limitation was not exceeded in the unconstrained case. In contrast, the change in the power generation profile of the HX scenarios reduced the accumulated revenue owing to the constraint on the maximum allowable deterioration. However, this reduction is almost negligible (0.11% in the HH scenario) because of the limited change in the operation profile and the mid-range prices where it occurred. This proves the suitability and advantages provided by the scheduling methodology presented in this work. The formulation of the scheduling problem with lifetime enhancement as a stochastic optimisation problem allows the limitation of damage in the equipment by modifying the power generation profiles where it has the largest effect on damage reduction and the minimum decrease in revenue. This is specially relevant when there is creep damage, as this deteriorating phenomena concentrates at specific periods of time where the operation of the thermal power plant originates high level of temperature and stress that may be largely reduced by small changes in the operation of the thermal power plant. Moreover, the intrinsic uncertainty attached to renewable energy sources can be included, and thus maximum profits can be achieved under different conditions.

4.2. Effect of design temperature on effective stress and creep damage

Creep damage depends on the temperature and stress of the equipment. Whilst the wall temperature is an absolute variable that only varies with the operation of the power plant, the thermal stresses that contribute to the effective stress are computed relatively to a design temperature where the material is free of this type of stress. Therefore, the damage of the power plant equipment is highly affected by its design temperature. Fig. 10 shows how the design temperature modifies the shape and magnitude of the effective stress in the unconstrained HH scenario. Higher design temperatures than that encountered in the wall of the superheater tubes generate inverse profiles of temperature and von Mises effective stress (see, e.g., the lines for 590 °C and 570 °C in Fig. 10). In contrast, the wall temperature and effective stress profiles follow the same tendency if the design temperature is lower than the wall temperature (see, e.g., the lines for 510 °C and 490 °C in Fig. 10). When the design temperature is between the maximum and minimum temperature of the wall for a given operation profile, the von Mises effective profile is a combination of both trajectories depending on whether the current wall temperature is above or below the design temperature (lines for 550 °C and 530 °C in Fig. 10).

Moreover, the inverse trajectories between the wall temperature and the effective stress for design temperatures above the maximum wall temperature reveal that the power generation profile that maximises the revenue also minimises the damage if there is a direct relation between the power generation and the wall temperature, i.e. more power leads to higher wall temperatures. When this condition is met and the design temperature of the equipment is above the peak of the wall temperature,

¹ In this context, unconstrained refers to the case where there is no limitation on the maximum damage. However, the remaining equality and inequality constraints are still included.

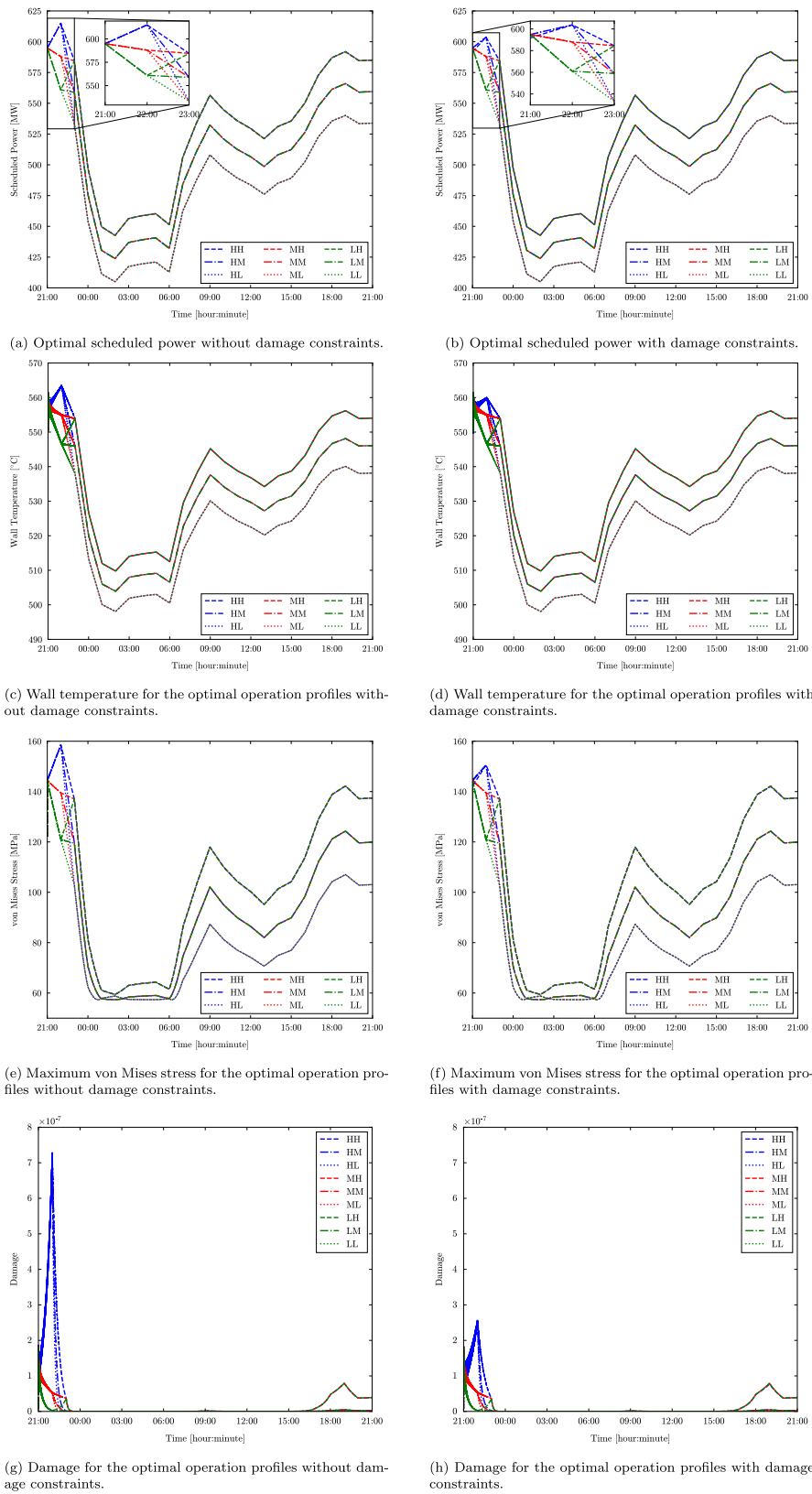


Fig. 7. Optimal scheduling of a flexible NGCC with and without damage limitation under uncertainty.

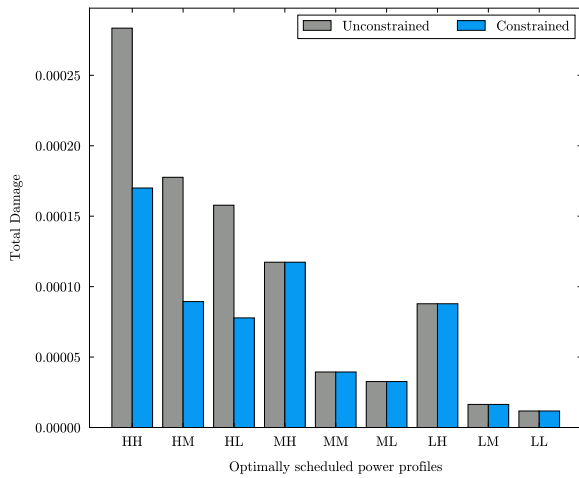


Fig. 8. Total creep damage in the tubes of the superheater for the different scenarios considered in the stochastic optimisation.

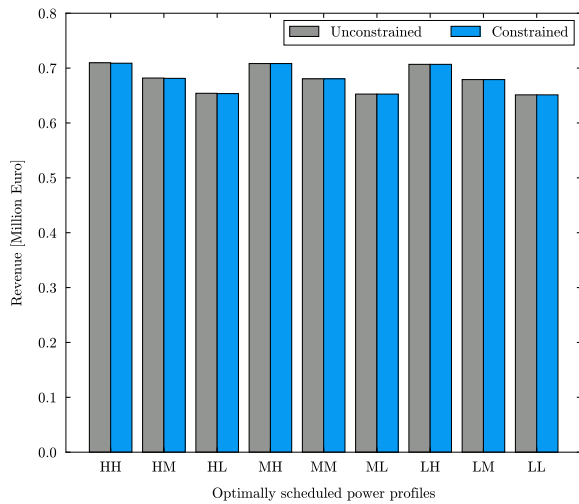


Fig. 9. Revenue for the different scenarios considered in the stochastic optimisation.

e.g. lines for 590 °C and 570 °C in Fig. 10, reducing the power generation leads to lower wall temperatures and thus higher temperature differences. As a result, the thermal stresses and the associated creep damage increase. Therefore, the optimal solution is the upper bound of the power generation, a limit where the creep damage cannot be further reduced. This solution does not hold if the wall temperature does not exhibit a proportional relation with the power generation, in which case the proposed methodology can find an operating profile that reduces the damage compared to the upper bound of the power generation.

The design temperature also influences the maximum value of the effective stress and temperature of the wall at which it occurs. Thus, the selection of an adequate design temperature can reduce notably the creep damage owing to the combined effect of these two variables. Table 3 compares the maximum effective stress value, the associated wall temperature at the instant it occurs and the accumulated damage, for three different scenarios and a broad range of design temperatures. These results demonstrate the trade-off existing between wall temperature and effective stress, since the lowest accumulated damage at each scenario occurred at the lowest combination of both variables, and not at

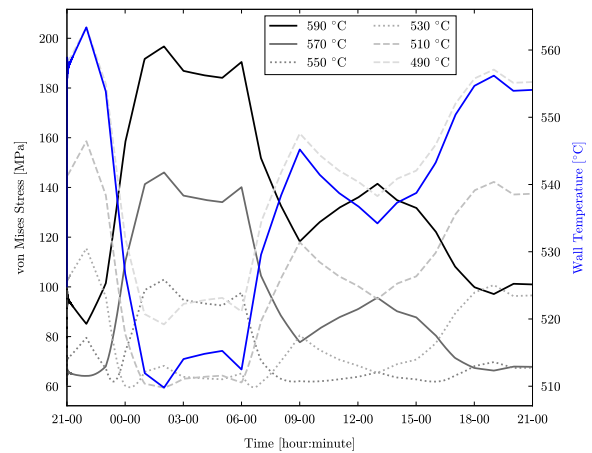


Fig. 10. Effective stress in the unconstrained HH scenario for different design temperatures. The maximum wall temperature for this scenario is included for shape comparison.

the smallest value of the maximum stress. Design temperatures closer to the highest wall temperature cause the maximum stress at the lowest wall temperatures because of the larger temperature difference (e.g. rows for design temperatures in the range 570–550 °C in Table 3), whilst design temperatures similar to the mean of the wall temperature reduce the overall temperature difference throughout the operation of the power plant but have the peak of stress at higher wall temperatures (rows 550–520 °C in Table 3).

5. Conclusions

Thermal power plants are expected to cycle more frequently and increase their number of start-ups and shut-downs in order to balance the intermittent power generation from renewable energy sources. In the long term, this type of operation may lead to larger deterioration of the equipment. Adequate scheduling of the power dispatched by flexible thermal power plants must hence consider the uncertainty associated to the increasing renewable energy sources whilst limiting the damage generated by the flexible operation of these thermal power units. This work seeks to address this challenge by proposing a methodology where the scheduling of power generation is formulated as a stochastic optimisation problem that considers the uncertainty in the power demand and limits the maximum deterioration of specific equipment.

Uncertainty in the power demand owing to the intermittent power generation of renewable energy sources was included in this methodology by formulating the scheduling problem as a scenario-tree based optimisation. This method considers several discrete realisations of the uncertainty associated to renewable power generation and combines them over time in a set of different scenarios that represent alternative profiles of power demand. Therefore, this optimisation problem aims at finding a set of optimal solutions that maximise the weighted sum of scenario revenues.

Deterioration of the equipment is embedded in the optimisation problem as a nonlinear constraint. This is achieved by a sequential procedure that calculates the damage over the considered operation time. During every iteration of the optimisation problem, the computed power generation profiles for each scenario are used to simulate the dynamic behaviour of the thermal power plant, which allows the estimation of temperature, pressure, stress and strain in specific equipment. Damage owing to different deterioration phenomena can subsequently be computed with these variables and experimental data. Since this is a general and sequential procedure, any damage mechanism (e.g. hot

Table 3

Effect of design temperature on the maximum effective stress, wall temperature at which occurs and total damage for different scenarios. Data for the HH scenario may be compared with Fig. 10.

T_{design} [°C]	HH			MM			LL		
	$\sigma_{\text{eff,max}}$ [MPa]	T_{wall} [°C]	Damage	$\sigma_{\text{eff,max}}$ [MPa]	T_{wall} [°C]	Damage	$\sigma_{\text{eff,max}}$ [MPa]	T_{wall} [°C]	Damage
590	196.75	509.77	$7.08 \cdot 10^{-5}$	210.39	503.92	$1.09 \cdot 10^{-4}$	224.13	498.07	$1.6 \cdot 10^{-4}$
570	146.09	509.77	$5.44 \cdot 10^{-7}$	159.19	503.92	$9.95 \cdot 10^{-7}$	172.50	498.07	$1.74 \cdot 10^{-6}$
560	123.98	509.77	$4.54 \cdot 10^{-8}$	136.61	503.92	$8.12 \cdot 10^{-8}$	149.57	498.07	$1.55 \cdot 10^{-7}$
550	102.96	509.77	$3.39 \cdot 10^{-8}$	114.82	503.92	$8.34 \cdot 10^{-9}$	127.22	498.07	$1.14 \cdot 10^{-8}$
540	96.12	563.34	$3.38 \cdot 10^{-7}$	94.38	503.92	$3.10 \cdot 10^{-8}$	105.84	498.07	$9.21 \cdot 10^{-9}$
530	115.53	563.34	$3.84 \cdot 10^{-6}$	104.35	554.72	$3.85 \cdot 10^{-7}$	104.23	554.65	$1.09 \cdot 10^{-7}$
520	136.57	563.34	$3.68 \cdot 10^{-5}$	124.14	554.72	$4.34 \cdot 10^{-6}$	124.02	554.65	$1.26 \cdot 10^{-6}$
510	158.60	563.34	$2.84 \cdot 10^{-4}$	144.92	554.72	$3.94 \cdot 10^{-5}$	144.79	554.65	$1.17 \cdot 10^{-5}$
500	181.32	563.34	$1.77 \cdot 10^{-3}$	168.60	562.40	$2.86 \cdot 10^{-4}$	168.40	562.32	$8.74 \cdot 10^{-5}$
490	204.46	563.34	$9.22 \cdot 10^{-3}$	192.95	562.40	$1.70 \cdot 10^{-3}$	192.74	562.32	$5.30 \cdot 10^{-4}$

corrosion, vibration, erosion, oxidation) can be included if the necessary variables to estimate the deterioration of the component can be obtained from the dynamic simulation of the thermal power plant.

Scheduling of a flexible natural gas combined cycle with limitation of creep damage in the tubes of the superheater demonstrated that the proposed methodology can enhance the lifetime operation of critical equipment by controlling its deterioration whilst maximising the economic revenue. This was achieved by modifying the set of power generation profiles in the time periods where the smaller changes in operation and revenue generation lead to the largest reduction in the damage. Therefore, the application of the proposed methodology to thermal power plants in deregulated power markets with a large deployment of renewable energy sources can enhance their lifetime with minimal detriment in the revenue.

The scheduling of the NGCC showed that the design temperature of the material notably affected the creep damage in the equipment. A comparison of its effect on the maximum effective stress, wall temperature and deterioration for a broad range of temperatures demonstrated that design temperatures close to the mean and peak values of the wall temperature in the tubes of the superheater substantially reduce the total damage generated by a given power generation profile, provided that the wall temperature and power generation are directly related (i.e. both increase or decrease simultaneously). In contrast, design temperatures larger than the maximum wall temperature lead to the trivial solution where the maximum power generation minimises the overall creep damage.

These results highlight the benefit of the scheduling methodology proposed in this work. Damage can be limited and controlled with minor

modifications on the scheduled power generation profile and economic revenue, which enhances the operational lifetime and profitability of the power units. Furthermore, this methodology may ease the selection of adequate design temperatures of materials for critical equipment in the design phase of the thermal power plant. Scheduling of start-ups and shut-downs can also be carried out provided they can be simulated within the optimisation framework.

Declaration of Competing Interest

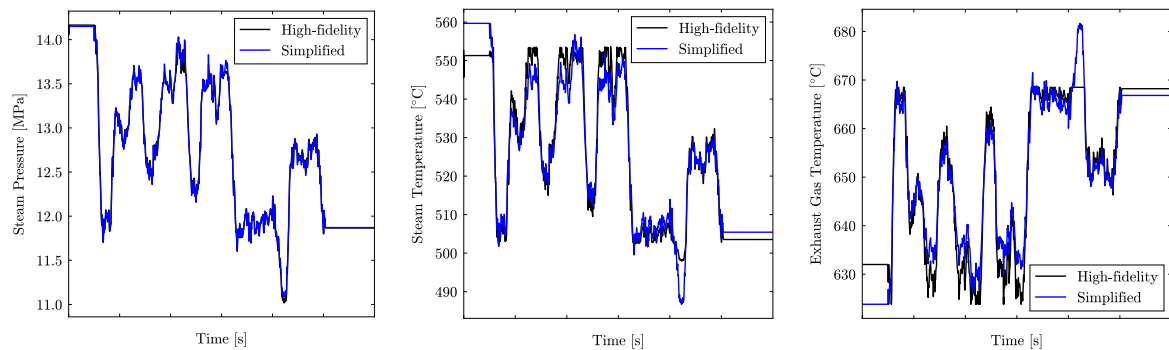
The authors declare that they have no known competing financial interests or personal relationships that could have appeared to influence the work reported in this paper.

Acknowledgements

This work has been financially supported by the Department of Energy and Process Engineering at the Norwegian University of Science and Technology - NTNU. The authors also thank Dr. Rubén Mochofí Montañés for providing the dynamic model of the power plant.

Appendix A. Model validation

This section presents the validation results of the models developed throughout this work. Fig. A.11 compares the high-fidelity and simplified models for the considered temperatures and pressure, whereas Fig. A.12 shows the agreement between the stresses and strains of the proposed models and the FEM analysis.



(a) Pressure of the steam inside the superheating tubes. (b) Temperature of the steam inside the superheating tubes. (c) Temperature of the exhaust gas outside the superheating tubes.

Fig. A.11. Comparison between the high-fidelity and simplified model predictions.

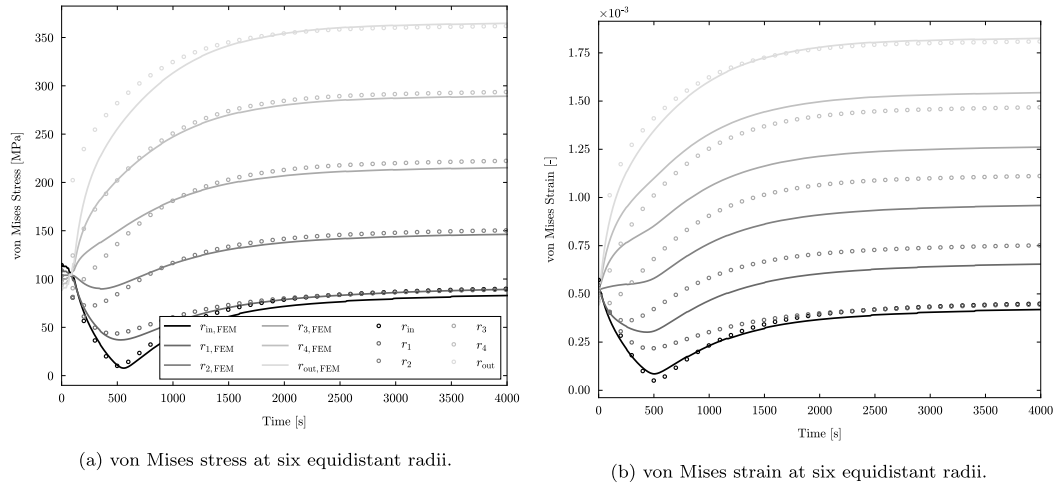


Fig. A.12. Validation of stress and strain models under the assumption of plain strain.

Appendix B. Power demand and price

Fig. B.13 presents the day-ahead demand profile used in the case study in Section 4, its coarse simplification, and the deterministic electricity price throughout the considered scheduling range.

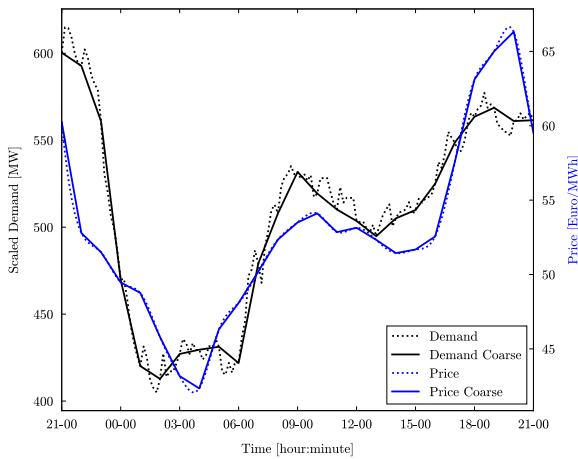


Fig. B.13. Demand profile estimated in day-ahead markets with a coarse simplification and deterministic electricity prices.

References

[1] IPCC, Summary for Policymakers. In: Global warming of 1.5C. An IPCC Special Report on the impacts of global warming of 1.5C above pre-industrial levels and related global greenhouse gas emission pathways, in the context of strengthening the global response to the threat of climate change, sustainable development, and efforts to eradicate poverty, [V. Masson-Delmotte, P. Zhai, H.O. Pörtner, D. Roberts, J. Skea, P.R. Shukla, A. Pirani, W. Moufouma-Okia, C.Péan, R. Pidcock, S. Connors, J.B.R. Matthews, Y. Chen, X. Zhou, M.I. Gomis, E. Lonnoy, T. Maycock, M. Tignor, T. Waterfield (eds.)]. World Meteorological Organization, Geneva, Switzerland, 2018.

[2] IEA, World Energy Outlook 2019: Executive Summary, <https://iea.blob.core.windows.net/assets/1f6bf453-3317-4799-ae7b-9cc6429c81d8/English-WE0-2019-ES.pdf>, 2019.

[3] J. Oswald, M. Raine, H. Ashraf-Ball, Will British weather provide reliable electricity? Energy Policy 36 (8) (2008) 3212–3225.

[4] M. Huber, D. Dimkova, T. Hamacher, Integration of wind and solar power in Europe: Assessment of flexibility requirements, Energy 69 (2014) 236–246.

[5] J. Bertsch, C. Growitsch, S. Lorenczik, S. Nagl, Flexibility in Europe’s power sector: An additional requirement or an automatic complement? Energy Econ. 53 (2016) 118–131.

[6] P. Eser, N. Chokani, R. Abhari, Operational and financial performance of fossil fuel power plants within a high renewable energy mix, J. Global Power Propul. Soc. 1 (2017) 16–27.

[7] M.A. González-Salazar, T. Kirsten, L. Prchlik, Review of the operational flexibility and emissions of gas-and coal-fired power plants in a future with growing renewables, Renew. Sustain. Energy Rev. 82 (2017) 1497–1513.

[8] J. Rúa, M. Bui, L.O. Nord, N. Mac Dowell, Does CCS reduce power generation flexibility? A dynamic study of combined cycles with post-combustion CO₂ capture, Int. J. Greenhouse Gas Control 95 (2020) 102984.

[9] R.M. Montañés, M. Korpás, L.O. Nord, S. Jaehnert, Identifying operational requirements for flexible CCS power plant in future energy systems, Energy Proc. 86 (2016) 22–31.

[10] H. Kondziella, T. Bruckner, Flexibility requirements of renewable energy based electricity systems—a review of research results and methodologies, Renew. Sustain. Energy Rev. 53 (2016) 10–22.

[11] R. Viswanathan, Damage mechanisms and life assessment of high temperature components, ASM International, 1989.

[12] R. Viswanathan, J. Stringer, Failure mechanisms of high temperature components in power plants, J. Eng. Mater. Technol. 122 (3) (2000) 246–255.

[13] T. Kim, D. Lee, S. Ro, Analysis of thermal stress evolution in the steam drum during start-up of a heat recovery steam generator, Appl. Therm. Eng. 20 (11) (2000) 977–992.

[14] F. Alobaid, R. Postler, J. Ströhle, B. Epple, H.-G. Kim, Modeling and investigation start-up procedures of a combined cycle power plant, Appl. Energy 85 (12) (2008) 1173–1189.

[15] S.C. Gülen, K. Kim, Gas turbine combined cycle dynamic simulation: a physics based simple approach, J. Eng. Gas Turbines Power 136 (1) (2014) 011601.

[16] P. Dzierwa, J. Taler, Optimum heating of pressure vessels with holes, J. Pressure Vessel Technol. 137 (1) (2015) 011202.

[17] J. Taler, P. Dzierwa, D. Taler, P. Harchut, Optimization of the boiler start-up taking into account thermal stresses, Energy 92 (2015) 160–170.

[18] F. Alobaid, N. Mertens, R. Starkloff, T. Lanz, C. Heinze, B. Epple, Progress in dynamic simulation of thermal power plants, Prog. Energy Combust. Sci. 59 (2017) 79–162.

[19] A.B. Ata, F. Alobaid, C. Heinze, A. Almoshih, A. Sanfeliu, B. Epple, Comparison and validation of three process simulation programs during warm start-up procedure of a combined cycle power plant, Energy Convers. Manage. 207 (2020) 112547.

[20] J. Rúa, R. Agromayor, M. Hillestad, L.O. Nord, Optimal dynamic operation of natural gas combined cycles accounting for stresses in thick-walled components, Appl. Therm. Eng. 170 (2020) 114858.

[21] J. Rúa, L.O. Nord, Optimal control of flexible natural gas combined cycles with stress monitoring: Linear vs nonlinear model predictive control, Appl. Energy 265 (2020) 114820.

[22] R. Viswanathan, W. Bakker, Materials for ultrasupercritical coal power plants—Boiler materials: Part I, J. Mater. Eng. Perform. 10 (1) (2001) 81–95.

[23] R. Viswanathan, W. Bakker, Materials for ultrasupercritical coal power plants—Turbine materials: Part II, J. Mater. Eng. Perform. 10 (1) (2001) 96–101.

[24] S. Suresh, Fatigue of materials, Cambridge University Press, 1998.

[25] N. Mukhopadhyay, S.G. Chowdhury, G. Das, I. Chattoraj, S. Das, D. Bhattacharya, An investigation of the failure of low pressure steam turbine blades, Eng. Fail. Anal. 5 (3) (1998) 181–193.

[26] S. Barella, M. Bellogini, M. Boniardi, S. Cincera, Failure analysis of a steam turbine rotor, Eng. Fail. Anal. 18 (6) (2011) 1511–1519.

[27] G. Das, S.G. Chowdhury, A.K. Ray, S.K. Das, D.K. Bhattacharya, Turbine blade failure in a thermal power plant, Eng. Fail. Anal. 10 (1) (2003) 85–91.

[28] I. Paterson, J. Wilson, Use of damage monitoring systems for component life optimisation in power plant, Int. J. Pressure Vessels Piping 79 (8–10) (2002) 541–547.

[29] P. Wang, L. Cui, M. Lyschik, A. Scholz, C. Berger, M. Oechsner, A local extrapolation based calculation reduction method for the application of constitutive material models for creep fatigue assessment, Int. J. Fatigue 44 (2012) 253–259.

- [30] A. Benato, A. Stoppato, S. Bracco, Combined cycle power plants: A comparison between two different dynamic models to evaluate transient behaviour and residual life, *Energy Convers. Manage.* 87 (2014) 1269–1280.
- [31] A. Benato, A. Stoppato, A. Mirandola, Dynamic behaviour analysis of a three pressure level heat recovery steam generator during transient operation, *Energy* 90 (2015) 1595–1605.
- [32] A. Benato, S. Bracco, A. Stoppato, A. Mirandola, Dynamic simulation of combined cycle power plant cycling in the electricity market, *Energy Convers. Manage.* 107 (2016) 76–85.
- [33] D. Ghosh, H. Roy, S. Ray, A. Shukla, High temperature corrosion failure of a secondary superheater tube in a thermal power plant boiler, *High Temp. Mater. Process.* 28 (1–2) (2009) 109–114.
- [34] N. Mukhopadhyay, B. Dutta, H. Kushwaha, On-line fatigue-creep monitoring system for high-temperature components of power plants, *Int. J. Fatigue* 23 (6) (2001) 549–560.
- [35] A.Y. Saber, G.K. Venayagamoorthy, Resource scheduling under uncertainty in a smart grid with renewables and plug-in vehicles, *IEEE Syst. J.* 6 (1) (2011) 103–109.
- [36] H. Pandžić, I. Kuzle, T. Čapuder, Virtual power plant mid-term dispatch optimization, *Appl. Energy* 101 (2013) 134–141.
- [37] S.M. Nosratabadi, R.-A. Hooshmand, E. Gholipour, A comprehensive review on microgrid and virtual power plant concepts employed for distributed energy resources scheduling in power systems, *Renew. Sustain. Energy Rev.* 67 (2017) 341–363.
- [38] R. Kehlhofer, F. Hannemann, B. Rukes, F. Stirnimann, *Combined-cycle gas & steam turbine power plants*, Pennwell Books, 2009.
- [39] *Thermoflow, GT Pro 24.0*, Thermoflow Inc, 2014.
- [40] Modelon, *Thermal Power Library*, <https://www.modelon.com/library/thermal-power-library/>, 2015.
- [41] Dassault Systemes, <https://www.3ds.com/products-services/catia/products/dymola/>, 2016.
- [42] Modelica Association, <https://www.modelica.org/>, 2019.
- [43] R.M. Montaños, S.Ó. GarDarsdóttir, F. Normann, F. Johnsson, L.O. Nord, Demonstrating load-change transient performance of a commercial-scale natural gas combined cycle power plant with post-combustion CO₂ capture, *Int. J. Greenhouse Gas Control* 63 (2017) 158–174.
- [44] L. Ljung, *System identification: theory for the user*, Prentice-hall, 1987.
- [45] S. Timoshenko, J.N. Goodier, *Theory of Elasticity*, McGraw-Hill book Company, 1951.
- [46] J. Schijve, Fatigue of structures and materials in the 20th century and the state of the art, *Int. J. Fatigue* 25 (8) (2003) 679–702.
- [47] M. Matsuishi, T. Endo, Fatigue of metals subjected to varying stress, *Japan Soc. Mech. Eng., Fukuoka, Japan* 68 (2) (1968) 37–40.
- [48] S.D. Downing, D.F. Socie, Simple rainflow counting algorithms, *Int. J. Fatigue* 4 (1) (1982) 31–40.
- [49] R. Sunder, S. Seetharam, T. Bhaskaran, Cycle counting for fatigue crack growth analysis, *Int. J. Fatigue* 6 (3) (1984) 147–156.
- [50] G. Marsh, C. Wignall, P.R. Thies, N. Barltrop, A. Incecik, V. Venugopal, L. Johanning, Review and application of rainflow residue processing techniques for accurate fatigue damage estimation, *Int. J. Fatigue* 82 (2016) 757–765.
- [51] M. Miner, Cumulative damage in fatigue, *J. Appl. Mech.* 12 (1945) A159–A164.
- [52] A. Fatemi, L. Yang, Cumulative fatigue damage and life prediction theories: a survey of the state of the art for homogeneous materials, *Int. J. Fatigue* 20 (1) (1998) 9–34.
- [53] D.F. Socie, *Multiaxial fatigue damage models*, *J. Eng. Mater. Technol.*
- [54] B.-R. You, S.-B. Lee, A critical review on multiaxial fatigue assessments of metals, *Int. J. Fatigue* 18 (4) (1996) 235–244.
- [55] S. Lucia, T. Finkler, S. Engell, Multi-stage nonlinear model predictive control applied to a semi-batch polymerization reactor under uncertainty, *J. Process Control* 23 (9) (2013) 1306–1319.
- [56] D. Krishnamoorthy, B. Foss, S. Skogestad, Real-time optimization under uncertainty applied to a gas lifted well network, *Processes* 4 (4) (2016) 52.
- [57] D. Krishnamoorthy, B. Foss, S. Skogestad, A distributed algorithm for scenario-based model predictive control using primal decomposition, *IFAC-PapersOnLine* 51 (18) (2018) 351–356.
- [58] M. Thombre, Z. Mdoe, J. Jäschke, Data-driven robust optimal operation of thermal energy storage in industrial clusters, *Processes* 8 (2) (2020) 194.
- [59] D. Kraft, A software package for sequential quadratic programming, *Forschungsbericht- Deutsche Forschungs- und Versuchsanstalt für Luft- und Raumfahrt*.
- [60] D. Kraft, Algorithm 733: Tomp–fortran modules for optimal control calculations, *ACM Trans. Math. Software (TOMS)* 20 (3) (1994) 262–281.
- [61] Steven G. Johnson, *The NLOpt nonlinear-optimization package*, <http://github.com/stevengj/nlopt>.
- [62] S. Spigarelli, E. Cerri, P. Bianchi, E. Evangelista, Interpretation of creep behaviour of a 9Cr–Mo–Nb–V–N (T91) steel using threshold stress concept, *Mater. Sci. Technol.* 15 (12) (1999) 1433–1440.